Ordering of hard needles at a hard wall

A. Poniewierski
Institute of Physical Chemistry, Polish Academy of Sciences, Kasprzaka 44/52, Warsaw 01-224, Poland
(Received 9 November 1992)

We study a system of hard spherocylinders in contact with a hard wall, assuming that the length-to-width ratio of the spherocylinder tends to infinity. The Onsager approximation is applied to calculate the free energy of the system. The integral equation for the one-particle distribution function is solved in the uniaxial case, i.e., for bulk densities corresponding to the isotropic phase. We find the density and order parameter profiles and conclude that the particles prefer parallel alignment close to the wall. Finally, we study the stability of the uniaxial solution and find the bifurcation point corresponding to the nematic order close to the wall.

PACS number(s): 61.30.Gd, 64.70.Md

I. INTRODUCTION

The problem of ordering of anisotropic liquid-crystal molecules at various surfaces attracts much experimental and theoretical interest [1,2]. The microscopic mechanism of ordering (or disordering) effects of the surface or interface on liquid crystals is quite complicated and still not very well understood although some progress has been made during recent years. For example, some solid substrates induce homeotropic, i.e., normal to the surface, nematic alignment whereas others favor alignment parallel to the surface of the substrate. Special preparation of the surface can even produce a tilt of the nematic director.

To understand qualitatively the behavior of liquid crystals in contact with a solid substrate or at an interface, one can apply the Landau–de Gennes theory [3–6]. However, in this case the orientational order parameter is a tensor and the number of phenomenological parameters of the theory becomes quite large when the surface interaction is added to the usual Landau–de Gennes Hamiltonian. This makes the analysis of all possible cases very difficult. The number of parameters can be reduced if a molecular theory is used. Moreover, the Landau–de Gennes theory seems unable to explain some experimental observations such as the tilt of the director at the nematic-isotropic interface [7] or the smectic-A order induced by a free surface of the isotropic phase of some compounds [8]. To study these phenomena, density-functional theories [9–11] or lattice models [12] are more appropriate.

As the real interaction between liquid-crystal molecules and a solid substrate can be quite complicated, in this paper we study a highly idealized situation of hard needles in contact with a hard wall. In 1949 Onsager [12] demonstrated that hard spherocylinders can undergo the nematic-isotropic transition when the length-to-width ratio L/D becomes very large. He also argued that the excess free energy of the system is then given by the second-order term of the virial expansion and all higher-order terms can be neglected. Strictly speaking the Onsager theory is valid in the limit $L/D \to \infty$, i.e., the hard needle limit, but it is often applied also for finite values of L/D. Extension of the Onsager theory to nonuniform fluids is straightforward and it has been used to study the nematic-isotropic interface [9,10]. Despite some discrepancies between different approaches to the problem it seems that the Onsager theory is capable of explaining the tilt of the director at the nematic-isotropic interface, at least in some range of L/D ratios. The same model has also been applied to study, in an approximate way, the nematic alignment at a solid substrate [14].

In this paper we undertake more detailed studies of the alignment of hard needles close to the wall when the isotropic phase is assumed in the bulk. In particular, we study the possibility of a surface transition in which the rotational symmetry in the plane of the wall is broken. Such a transition is likely to occur if the wall favors the parallel alignment of hard needles and their concentration approaches the critical value at which the bulk isotropic-to-nematic transition takes place.

The plan of the paper is as follows. In Sec. II we recall the Onsager theory for nonuniform systems and obtain an integral equation for the one-particle distribution function in the limit $L/D \to \infty$. The results of numerical solutions of that equation in the case of uniaxial symmetry and the comparison with the pressure sum rule are presented in Sec. III. In Sec. IV we study the stability of the uniaxial solution in order to locate the surface transition to the biaxial phase, and Sec. V is devoted to the discussion.

II. THEORY

We consider a system of hard spherocylinders of length L and diameter D in contact with a hard and structureless wall. The grand canonical potential of the system, Ω, can be expressed as a functional of the one-particle distribution function $\rho(z,\omega)$ [15], where $z \geq 0$ measures the distance of the particle center of mass from the wall and $\omega=(\vartheta,\phi)$ denotes its orientation. In the Onsager approximation, Ω is given by

$$\beta\Omega/A=\int_0^\infty dz\,d\omega\,\rho(z,\omega)[\ln\Lambda^3\rho(z,\omega)-1]-\beta\mu\int_0^\infty dz\,d\omega\,\rho(z,\omega)+\tfrac{1}{2}\int_0^\infty dz_1 d\omega_1\int_0^\infty dz_2 d\omega_2 V(z_{12},\omega_1,\omega_2)\times\rho(z_1,\omega_1)\rho(z_2,\omega_2)\ , \tag{2.1}$$

where $V(z_{12},\omega_1,\omega_2)=-\int d\mathbf{r}_{12}^{\perp} f_2(\mathbf{r}_{12},\omega_1,\omega_2)$, β is the Boltzmann factor, A is the area of the wall, Λ is the thermal de Broglie wavelength, and f_2 denotes the Mayer function for hard spherocylinders. Because of the presence of the wall $\rho(z,\omega)$ must vanish if $z<z_{\min}(\omega)=\frac{1}{2}(L|\cos\vartheta|+D)$. We assume that at $z=+\infty$ the system is isotropic and its density is equal to ρ_b, i.e., $\rho(+\infty,\omega)=\rho_b/4\pi$. The excluded volume for hard spherocylinders is given by $V_0(\vartheta_{12})=2L^2D\sin\vartheta_{12}+2\pi LD^2+\frac{4}{3}\pi D^3$ and when the ratio L/D is large only the first term is important and the remaining two terms can be neglected. Using this approximation for V_0 one finds the following relation between μ and ρ_b:

$$\beta\mu\cong\ln(\Lambda^3\rho_b/4\pi)+\frac{\pi}{2}L^2D\rho_b\ . \tag{2.2}$$

Minimization of Ω with respect to $\rho(z,\omega)$ together with Eq. (2.2) leads to the following integral equation:

$$\ln[4\pi\rho(z_1,\omega_1)/\rho_b]+\int_0^\infty dz_2 d\omega_2 V(z_{12},\omega_1,\omega_2)\times\rho(z_2,\omega_2)-\frac{\pi}{2}L^2D\rho_b=0\ . \tag{2.3}$$

Our aim is to solve this equation in the case of extremely elongated spherocylinders. Therefore we use in (2.3) $V(z_{12},\omega_1,\omega_2)$ obtained in the limit $L/D\to\infty$. To perform this limit, we note first that $V(z_{12},\omega_1,\omega_2)$ can be conveniently expressed as follows:

$$V(z_{12},\omega_1,\omega_2)=-\int d\mathbf{r}\,\delta(z_{12}-\hat{\mathbf{k}}\cdot\mathbf{r})f_2(\mathbf{r},\omega_1,\omega_2)\ , \tag{2.4}$$

where $\hat{\mathbf{k}}$ is a unit vector normal to the wall and $\delta(x)$ denotes the Dirac δ function. Up to the leading order in L/D, the integration is performed over the parallelepiped defined as a set of points $\mathbf{r}=\frac{1}{2}r_1L\hat{\boldsymbol{\omega}}_1+\frac{1}{2}r_2L\hat{\boldsymbol{\omega}}_2+r_3D[(\hat{\boldsymbol{\omega}}_1\times\hat{\boldsymbol{\omega}}_2)/\sin\vartheta_{12}]$, for which $|r_i|\le 1$, $i=1,2,3$ and $\hat{\boldsymbol{\omega}}_j=(\sin\vartheta_j\cos\phi_j,\sin\vartheta_j\sin\phi_j,\cos\vartheta_j)$, $j=1,2$. The change of the integration variables in (2.4) gives

$$V(z_{12},\omega_1,\omega_2)=\tfrac{1}{4}L^2D\sin\vartheta_{12}\int_{-1}^1 dr_1\int_{-1}^1 dr_2\int_{-1}^1 dr_3\,\delta\left[z_{12}-\tfrac{1}{2}r_1L\hat{\omega}_1\cdot\hat{\mathbf{k}}-\tfrac{1}{2}r_2L\hat{\omega}_2\cdot\hat{\mathbf{k}}-r_3D\frac{(\hat{\boldsymbol{\omega}}_1\times\hat{\boldsymbol{\omega}}_2)\cdot\hat{\mathbf{k}}}{\sin\vartheta_{12}}\right]\ . \tag{2.5}$$

In the rest of the paper we assume that L is the unit of length. Then the limit $L/D\to\infty$ is equivalent to $D\to 0$. If we take this limit in (2.5) the integration over r_3 can be performed and (2.3) can be rewritten in terms of dimensionless quantities as follows:

$$\ln n(z_1,\omega_1)+\frac{\lambda}{4\pi}\int_0^\infty dz_2 d\omega_2 V(z_{12},\omega_1,\omega_2)\times n(z_2,\omega_2)-\frac{\pi}{2}\lambda=0\ , \tag{2.6}$$

where $\lambda=L^2D\rho_b$ and $n(z,\omega)=4\pi\rho(z,\omega)/\rho_b$. The kernel of the integral is given now by

$$V(z_{12},\omega_1,\omega_2)=\tfrac{1}{2}\sin\vartheta_{12}\times\int_{-1}^1 dr_1\int_{-1}^1 dr_2\,\delta(z_{12}-\tfrac{1}{2}r_1u_1-\tfrac{1}{2}r_2u_2)\ , \tag{2.7}$$

where $u_i=\hat{\boldsymbol{\omega}}_i\cdot\hat{\mathbf{k}}=\cos\vartheta_i$, $i=1,2$. Note that the integral in (2.7) does not depend on the signs of u_1 and u_2. The dimensionless parameter λ is the suitable measure of concentration of very thin hard rods in the Onsager theory. This theory predicts that the nematic-isotropic transition occurs when $\lambda=\lambda_I=4.19$ and its value jumps to $\lambda=\lambda_N=5.34$ in the nematic phase; the nematic order parameter at the transition is $Q=0.79$.

It is convenient to introduce a new variable, $\zeta=z-\frac{1}{2}|u|$, which measures the distance from the wall of the end of the particle closer to the wall. We also define the distribution of the ends as $\mathbf{n}_e(\zeta,\omega)=n(\zeta+\frac{1}{2}|u|,\omega)$. The advantage of such a choice of variables is that ζ changes from 0 to ∞ independently of ω despite the presence of the hard wall. Using the new variables we transform (2.7) into

$$V(\zeta_{12},\omega_1,\omega_2)=2\sin\vartheta_{12}\int_0^1 dr_1'\int_0^1 dr_2'\,\delta(\zeta_2+r_2'|u_2|-\zeta_1-r_1'|u_1|)=\frac{2\sin\vartheta_{12}}{|u_1u_2|}\int_{\zeta_1}^{\zeta_1+|u_1|}dt_1\int_{\zeta_2}^{\zeta_2+|u_2|}dt_2\,\delta(t_2-t_1)\ , \tag{2.8}$$

where $\zeta_{12}=\zeta_2-\zeta_1$, $r_1'=(1+r_1)/2$, $r_2'=(1-r_2)/2$, and $t_i=\zeta_i+r_i'|u_i|$, $i=1,2$. Combining (2.6) and (2.8) we find that

$$\ln n_e(\zeta_1,\omega_1)+\frac{\lambda}{4\pi}\int d\omega_2 2\sin\vartheta_{12}\frac{1}{|u_1|}\times\int_{\zeta_1}^{\zeta_1+|u_1|}dt\,N(t,\omega_2)-\frac{\pi}{2}\lambda=0\ , \tag{2.9}$$

where

$$N(t,\omega)=\begin{cases}\dfrac{1}{|u|}\displaystyle\int_0^t n_e(\zeta,\omega)d\zeta & \text{if } t<|u|\\ \dfrac{1}{|u|}\displaystyle\int_{t-|u|}^t n_e(\zeta,\omega)d\zeta & \text{if } t>|u|\ .\end{cases} \tag{2.10}$$

In this section we restrict our considerations to the distribution functions of uniaxial symmetry with respect to the z axis. This means that the distribution of the ends depends only on ζ and u; in addition $n_e(\zeta,u)=n_e(\zeta,-u)$. To perform integration over the angles in (2.9), we expand $\sin\vartheta_{12}$ in a series of the Legendre polynomials, P_l, as follows:

$$\sin\vartheta_{12}=\sum_{l=0}^{\infty}s_l P_l(\cos\vartheta_{12})\ , \tag{2.11}$$

where $s_l=0$ if l is odd. Substituting (2.11) into (2.9) and applying the addition theorem we obtain

$$\ln n_e(\zeta,u)+2\lambda\sum_{l=0}^{\infty}s_l P_l(u)\frac{1}{|u|}\times\int_{\zeta}^{\zeta+|u|}dt\,N_l(t)-\frac{\pi}{2}\lambda=0\ , \tag{2.12}$$

where the functions $N_l(t)$, for $l=0,2,4,\ldots$ are defined as follows:

$$N_l(t)=\frac{1}{4\pi}\int P_l(u)N(t,u)d\omega$$

$$=\begin{cases}\displaystyle\int_0^t d\zeta\int_{t-\zeta}^1\frac{du}{u}P_l(u)n_e(\zeta,u) & \text{if } t<1\\ \displaystyle\int_{t-1}^t d\zeta\int_{t-\zeta}^1\frac{du}{u}P_l(u)n_e(\zeta,u) & \text{if } t>1\ .\end{cases} \tag{2.13}$$

Taking the exponent of both sides of Eq. (2.12) we can determine self-consistently $N_l(t)$ from (2.12) and (2.13). Because $n_e(+\infty,u)=1$ we find from (2.13) that $N_l(+\infty)=\delta_{l0}$. In the opposite limit of $t\to0$, $N_l(t)\to0$ for all l. It is interesting to study the asymptotic behavior of $N_l(t)$ for $t\to0$ as we expect some nonanalyticity in this regime. Differentiating $N_l(t)$ we find that $N_l'(t)\sim-n_e(0^+,0)P_l(0)\ln t$, hence

$$N_l(t)\underset{t\to0}{\sim}n_e(0^+,0)P_l(0)t(1-\ln t)\ . \tag{2.14}$$

From Eqs. (2.14) and (2.12) we recover the asymptotic expression for $n_e(\zeta,u)$ when both ζ and u are small, i.e.,

$$\ln n_e(\zeta,u)\underset{\zeta,u\to0}{\sim}\frac{\pi}{2}\lambda-\frac{4\lambda}{\pi}n_e(0^+,0)\times\left\{\frac{1}{2|u|}[(\zeta+|u|)^2\ln(\zeta+|u|)-\zeta^2\ln\zeta]-\tfrac{3}{4}(|u|+2\zeta)\right\}\ , \tag{2.15a}$$

which gives

$$\ln n_e(\zeta,u=0)\underset{\zeta\to0}{\sim}\frac{\pi}{2}\lambda+\frac{4\lambda}{\pi}n_e(0^+,0)\zeta(\ln\zeta-1)\ , \tag{2.15b}$$

$$\ln n_e(\zeta=0^+,u)\underset{u\to0}{\sim}\frac{\pi}{2}\lambda+\frac{4\lambda}{\pi}n_e(0^+,0)|u|(\tfrac{1}{2}\ln|u|-\tfrac{3}{4})\ , \tag{2.15c}$$

where $\ln n_e(0^+,0)=\pi/2\lambda$. The last relation can be also expressed as $\ln\Lambda^3\rho(0^+,0)=\beta\mu$, which is the relation between the chemical potential and density for the ideal gas. It results from asymptotic relations (2.15) that the point $\zeta=u=0$ corresponds to a maximum of $n_e(\zeta,u)$ and the derivative of n_e in any direction is equal to $-\infty$ at this point. This singular behavior of the derivative of n_e results from the limit $D\to0$ and it concerns only one point $\zeta=u=0$. From Eqs. (2.15) we can also conclude that the particles close to the wall favor parallel alignment.

III. RESULTS

To solve Eq. (2.12), we have to determine $N_l(t)$ in a self-consistent manner from (2.12) and (2.13). It is convenient to redefine $N_0(t)$ by substituting into (2.13) $n_e(\zeta,u)-\delta_{10}$ instead of $n_e(\zeta,u)$. This is in order to have the same boundary conditions: $N_l(0)=N_l(+\infty)=0$ for all l. Then we assume that $N_l(t)$ can be truncated at some $t_{\max}$, i.e., $N_l(t)=0$ if $t>t_{\max}$: in our calculations $t_{\max}=2$ (in units of L). It is rather important to take into account the asymptotic behavior of $N_l(t)$ for $t\to0$. To do this, we assume that $N_l(t)=(1-\ln t)f_l(t)$, where the functions $f_l(t)$ satisfy the following conditions: $f_l(t)\sim t$ for $t\to0$ and $f_l(t_{\max})=0$. Then we expand $f_l(t)$ in a series of suitable orthogonal functions $\psi_k(t)$, $k=0,1,2,\ldots$ defined for $0\le t\le t_{\max}$. We choose

$$\psi_k(t)=\left[\frac{(2k+5)k!}{t_{\max}(k+4)!}\right]^{1/2}P_{k+2}^2\left[\frac{2t-t_{\max}}{t_{\max}}\right]\ , \tag{3.1}$$

where $P_{k+2}^2(x)$ is an associated Legendre polynomial. It results from the definition that $\psi_k(t_{\max})=0$, $\psi_k(t)\sim t$ for $t\to0$, and

$$\int_0^{t_{\max}}\psi_k(t)\psi_{k'}(t)dt=\delta_{kk'}\ .$$

Then the expansion $f_l(t)=\sum_{k\ge0}f_{lk}\psi_k(t)$ is substituted into Eqs. (2.12) and (2.13) from which the coefficients f_{lk} can be determined self-consistently. We note that all $N_l(t)$ are approximated by smooth functions, which is not compatible with definition (2.13). However, it is easy to

TABLE I. Comparison of the pressure sum rule $\int_0^1 n_e(0^+,u)du = 1+\pi\lambda/4$ [see Eqs. (3.2) and (3.3)] with the results of numerical calculations. Note that for $\lambda > 3.55$ the uniaxial solution is unstable.

λ	$1+\pi\lambda/4$	$\int_0^1 n_e(0^+,u)du$
1.0	1.785	1.786
2.0	2.571	2.586
3.0	3.356	3.470
3.5	3.749	4.079
4.0	4.142	4.789
4.1	4.220	5.101
4.15	4.259	5.270

check that the functions $N_l(t)$ and their first derivatives are continuous at $t=1$, and a discontinuity may occur only in higher derivatives. Therefore we do not expect any serious consequences of our approximation, especially that all $N_l(t)$ are rather small in the region $1 \le t \le t_{\max}$. We have solved Eq. (2.12) for $\lambda = 1$, 2, 3, 3.5, 4, 4.1, and 4.15 using the coefficients f_{lk} as independent variables, for $0 \le l \le l_{\max}$ and $0 \le k \le k_{\max}$, where $l_{\max}=10$ and $k_{\max}$ up to 30 have been used. The solutions have been found with the aid of a minimizing procedure. We can compare our results with the exact pressure sum rule which the equilibrium one-particle distribution function should satisfy [16], i.e.,

$$\int \rho(z^+_{\min}(\omega),\omega)d\omega = \beta p \ , \tag{3.2}$$

where p denotes the bulk pressure. Application of (3.2) to our system gives

$$\int_0^1 n_e(0^+,u)du = 1+\frac{\pi}{4}\lambda \ . \tag{3.3}$$

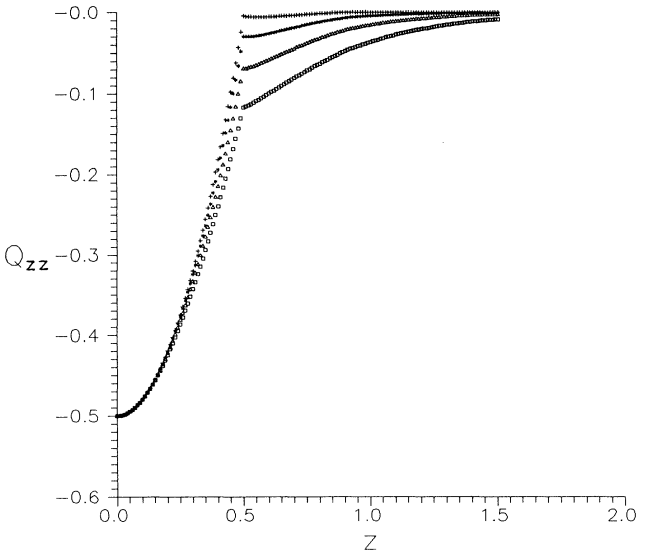

FIG. 2. $Q_{zz} = \langle P_2 \rangle$ component of the order parameter tensor vs the distance from the wall. P_2 is averaged with the one-particle distribution function for the centers of mass. Meaning of symbols and units the same as in Fig. 1.

The comparison of the exact relation (3.3) with the results of numerical calculations is presented in Table I. We note that for $\lambda \le 2$ the agreement is almost perfect whereas for higher values of λ it worsens gradually even though a quite large number of variables have been used to approximate the solution. We discuss this fact in the last section.

In Fig. 1 we plot the density $n(z) = \int n(z,u)d\omega/4\pi$ for a few values of λ. If $0 < z < \frac{1}{2}$ then $n(z) = \int_0^{2z} n(z,u)du$ and $n(z) \sim 2zn(0^+,0)$ when $z \to 0$. The first derivative of

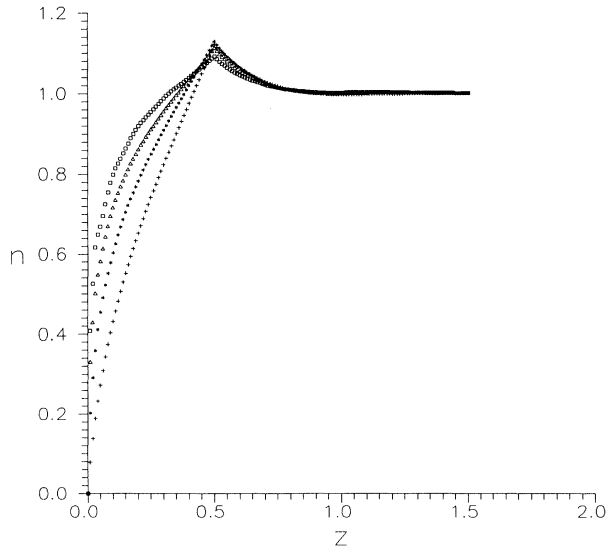

FIG. 1. Normalized density of the mass centers vs the distance from the wall (in units of L), for $\lambda=1$ (crosses), $\lambda=2$ (asterisks), $\lambda=3$ (triangles), and $\lambda=4$ (squares).

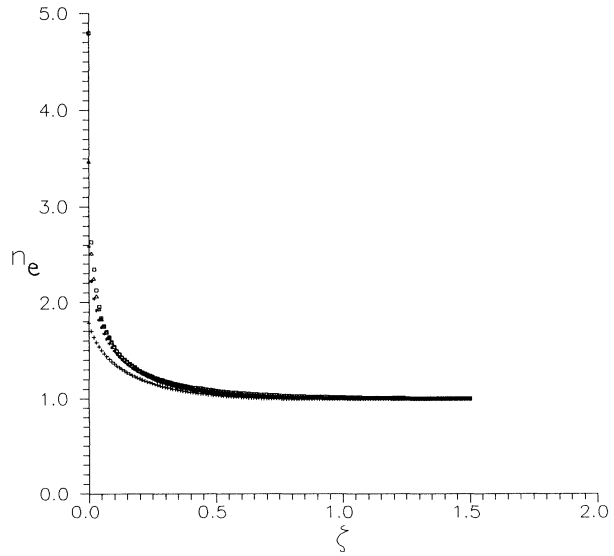

FIG. 3. Normalized density of the ends of the particles vs the distance from the wall. Meaning of symbols and units the same as in Fig. 1.

$n(z)$ must be discontinuous at $z=\frac{1}{2}$ because $n(z)=\int_0^1 n(z,u)du$ for $z>\frac{1}{2}$. We note that the kink at $z=\frac{1}{2}$ coincides with the maximum of $n(z)$. The maximum is only about 10% above the bulk value which is reached at $z\approx 1$. The order parameter in our problem is $Q_{zz}(z)=\int (d\omega/4\pi)n(z,u)P_2(u)/n(z)$ and it is plotted in Fig. 2. It results from the definition that $Q_{zz}(0^+)=-\frac{1}{2}$. We note that for small values of λ a very good approximation for $Q_{zz}(z)$ is obtained when $n(z,u)$ is approximated by the Heaviside step function, i.e., $n(z,u)\approx\Theta(z-\frac{1}{2}|u|)$. This approximation gives $Q_{zz}=2z^2-\frac{1}{2}$, for $z<\frac{1}{2}$ and $Q_{zz}=0$, otherwise. When λ increases the tail of $Q_{zz}(z)$ becomes more apparent and more slowly decaying than in the case of $n(z)$.

Replacing $n(z,u)$ by $n_e(\zeta,u)$ we define $n_e(\zeta)$ and $Q^e_{zz}(\zeta)$. The sum rule can be rewritten in the form resembling the case of spherical particles at a hard wall, i.e., $\rho_e(0^+)=\lambda n_e(0^+)=\beta p$. The concentration of the ends $n_e(\zeta)$ decreases and the order parameter $Q^e_{zz}(\zeta)$ increases monotonically with ζ without any kinks (see Figs. 3 and 4). We can conclude that in the context of anisotropic particles in contact with a hard wall the variables (ζ,u) are more convenient than (z,u). This is because in the former case the orientational and positional variables are always independent of each other whereas in the latter case they are coupled close to the wall.

Apart from the profile of the order parameter we also define the average surface order parameter:

$$\Gamma_{zz}=\frac{1}{4\pi}\int_0^\infty dz\,d\omega\,n(z,u)P_2(u)$$
$$=\frac{1}{4\pi}\int_0^\infty d\zeta\,d\omega\,n_e(\zeta,u)P_2(u)-\tfrac{1}{16}\ . \tag{3.4}$$

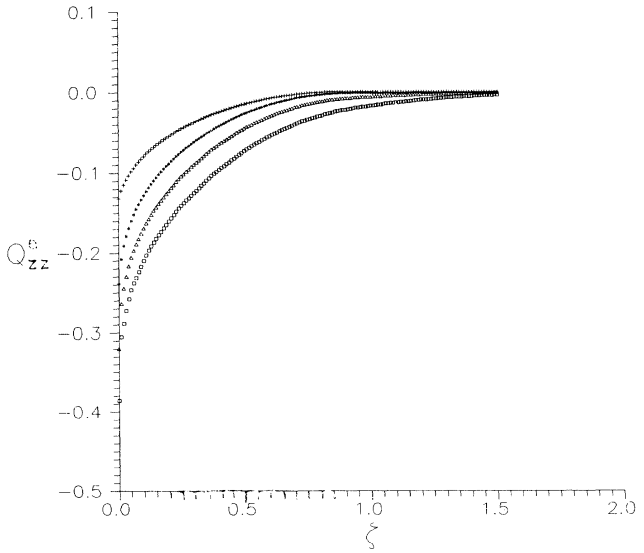

FIG. 4. $Q^e_{zz}=\langle P_2\rangle$ component of the order parameter tensor vs the distance from the wall. P_2 is averaged with the one-particle distribution function for the ends of the particles. Meaning of symbols and units the same as in Fig. 1.

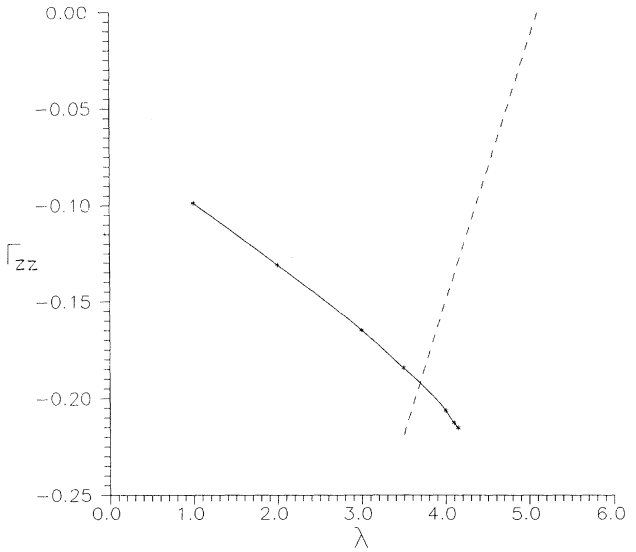

FIG. 5. Average surface order parameter vs the bulk density λ (solid line). The dashed line is defined by Eq. (4.5) (see text). The intersection of the two lines gives a rough estimate of the stability limit for the uniaxial solution.

It is a useful quantity to study the surface phase transition, which is shown in the next section. The plot of Γ_{zz} against λ is presented in Fig. 5.

IV. STABILITY ANALYSIS

The order parameter in our problem is a traceless tensor which in its diagonal form is given by

$$(Q_{ij})=\tfrac{1}{2}\langle 3\omega_i\omega_j-\delta_{ij}\rangle=\begin{bmatrix}-\frac{1}{2}Q+P & 0 & 0\\ 0 & -\frac{1}{2}Q-P & 0\\ 0 & 0 & Q\end{bmatrix}. \tag{4.1}$$

In a system of uniaxial symmetry, $Q_{zz}=Q\neq 0$ and $P=0$. Positive Q means that particles are on average aligned along the z axis whereas $Q<0$ corresponds to the situation when the orientations of particles are close to the xy plane. In the latter case, if the system is in the nematic phase there is some orientational order in the xy plane, i.e., the system is biaxial ($P\neq 0$). A negative Q can be achieved due to a bulk external field, which affects the nematic-isotropic transition [17], or a limiting surface. In the latter case, it has been shown in the framework of a Landau–de Gennes theory [5] that if the wall favors parallel alignment at the surface then a surface phase transition to a biaxial phase preceding the bulk isotropic-to-nematic transition can be expected.

We have already shown that the wall favors parallel alignment of hard needles. To locate the surface phase transition, we apply the stability analysis to the uniaxial solution of Eq. (2.12). In other words, we see the bifurcation point at which a biaxial solution branches off from the uniaxial solution.

It is helpful to consider first a simpler problem of a

bulk system of hard needles in an external field along the z axis. We assume that the system is in the paranematic phase, i.e., $Q\neq 0$ but small, and that the field induces negative Q. We can ask about the stability of the system with respect to the nematic perturbations in the xy plane. To find the critical value of λ at which the loss of stability occurs, we linearize the integral equation for the distribution function around the equilibrium distribution $f(u=\cos\vartheta)$ as follows:

$$\delta\rho(\omega_1)+2\lambda f(u_1)\int(\sin\vartheta_{12})\delta\rho(\omega_2)d\omega_2=0\ , \tag{4.2}$$

where

$$\int f(u)d\omega=1\ .$$

Applying (2.11) and the addition theorem we transform (4.2) into

$$\left[\delta_{ll'}+2\lambda\sum_{l'\geq|m|}s_{l'}\frac{4\pi}{2l'+1}V^m_{ll'}\right]\delta\rho^m_{l'}=0\ , \tag{4.3}$$

where

$$\delta\rho^m_l=\int\delta\rho(\omega)Y^m_l(\omega)^*d\omega\ ,$$

$$V^m_{ll'}=\int Y^m_l(\omega)^*Y^m_l(\omega)f(u)d\omega\ ,$$

and Y^m_l denotes a spherical harmonic. Because Q is small we can use the approximation $f(u)\approx[1+5QP_2(u)]/4\pi$. The bifurcation occurs when Eq. (4.3) has a nonzero solution. We take into account only terms linear in Q and therefore it is sufficient to consider only the diagonal components of the matrix appearing in (4.3). This leads to the following equation for the bifurcation point corresponding to the given l and m:

$$1+2\lambda\frac{s_l}{2l+1}(1+4\pi\sqrt{5/4\pi}Qv^m_{ll})=0\ , \tag{4.4}$$

where

$$v^m_{ll'}=\int d\omega\ Y^m_l(\omega)^*Y^m_{l'}(\omega)Y^0_2(\omega)\ .$$

We expect that the lowest value of λ satisfying Eq. (4.4) corresponds to $l=m=2$. Thus the loss of stability occurs at

$$\lambda=\lambda_c\approx\frac{16}{\pi}(1+\tfrac{10}{7}Q)\ . \tag{4.5}$$

In the absence of external fields, $Q=0$ and relation (4.5) gives simply the value of λ at which the isotropic phase becomes unstable with respect to the nematic perturbations proportional to P_2. For $Q<0$, the uniaxial phase becomes unstable with respect to the nematic (biaxial) perturbations proportional to Y^2_2 at a lower value of λ than in the case of $Q=0$.

Relation (4.5) can be applied to the present surface problem to obtain a rough estimate of the bifurcation point. The wall induces negative $Q_{zz}(z)$ and the thickness of the surface layer is approximately equal to L (see Fig. 2). Therefore it is reasonable to identify Q as Γ_{zz}. Then we superimpose the straight line $\lambda_c(Q)$ given by (4.5) on the plot of $\Gamma_{zz}(\lambda)$ (see. Fig. 5). The value of λ at which $\lambda_c(Q)$ crosses $\Gamma_{zz}(\lambda)$ is the approximate location of the surface bifurcation point $\lambda=\lambda^s_c$. We find that $\lambda^s_c\approx 3.69$, which corresponds to $Q=\Gamma_{zz}\approx -0.192$.

To calculate λ^s_c rigorously, we linearize Eq. (2.6) and express it in terms of $n_e(\zeta,u)$ as follows:

$$\delta n_e(\zeta_1,\omega_1)+\frac{\lambda}{4\pi}n^0_e(\zeta_1,u_1)\times\int_0^\infty d\zeta_2 d\omega_2 V(\zeta_{12},\omega_1,\omega_2)\delta n_e(\zeta_2,\omega_2)=0\ , \tag{4.6}$$

where $n^0_e(\zeta,u)$ is the uniaxial solution of Eq. (2.12) for the given value of λ and $\delta n_e(\zeta,\omega)$ denotes a biaxial perturbation. We seek the smallest value of λ at which Eq. (4.6) has a nontrivial solution. Using (2.8) and (2.11) we transform Eq. (4.6) into

$$\delta n^m_e(\zeta_1,u_1)+\lambda n^0_e(\zeta_1,u_1)\times\int_0^1 du_2\int_0^\infty d\zeta_2 V^m(\zeta_{12},u_1,u_2)\delta n^m_e(\zeta_2,u_2)=0\ , \tag{4.7}$$

where

$$V^m(\zeta_{12},u_1,u_2)=\frac{1}{2\pi}\int_0^{2\pi}d(\varphi_1-\varphi_2)V(\zeta_{12},\omega_1,\omega_2)\times e^{-im(\varphi_1-\varphi_2)}\ ,$$

$$\delta n^m_e(\zeta,u)=\frac{1}{2\pi}\int_0^{2\pi}d\varphi\,\delta n_e(\zeta,\omega)e^{-im\varphi}\ .$$

Because of the symmetries of the distribution function, $\delta n^m_e(\zeta,u)=0$ if m is odd. We could proceed in the same way as in the case of the nonlinear equation (2.12). However, in this context it is more convenient to expand the Dirac δ function appearing in (2.8), in a series of orthogonal functions defined by (3.1) as follows:

$$\delta(t_1-t_2)=\sum_k\psi_k(t_1)\psi_k(t_2)\ . \tag{4.8}$$

Using (2.8), (2.11), and (4.8) we find the following diagonal representation of V^m, for $|m|=2,4,6,\ldots$:

$$V^m(\zeta_{12},u_1,u_2)=-2\sum_{l\geq|m|}C^m_l P^{|m|}_l(u_1)P^{|m|}_l(u_2)\times\sum_k\Psi_k(\zeta_1,u_1)\Psi_k(\zeta_2,u_2)\ , \tag{4.9}$$

where

$$C^m_l=|s_l|\frac{(1-|m|)!}{(1+|m|)!},\quad \Psi_k(\zeta,u)=\frac{1}{u}\int_\zeta^{\zeta+u}\psi_k(t)dt$$

and we have used the fact that $s_l<0$ for $l\geq 2$. The substitution of (4.9) into (4.7) gives

$$\delta n^m_e(\zeta,u)-2\lambda n^0_e(\zeta,u)\sum_{l\geq|m|}(C^m_l)^{1/2}\sum_k\delta n^m_{lk}P^{|m|}_l(u)\times\Psi_k(\zeta,u)=0\ , \tag{4.10}$$

where

$$\delta n^m_{lk}=(C^m_l)^{1/2}\int_0^1 du\int_0^{\zeta_{\max}}d\zeta\,P^{|m|}_l(u)\Psi_k(\zeta,u)\delta n^m_e(\zeta,u)$$

and $\zeta_{\max}=t_{\max}$.

Equation (4.10) shows that δn^m_e can be expressed in terms of its projections onto functions $P^{|m|}_l\Psi_k$. Although these functions are not orthogonal to one another, they

are linearly independent nevertheless. Finally, we transform (4.10) into a set of linear equations for the projections δn_{lk}^m as follows:

$$\sum_{l'} \sum_{k'} A^m_{lkl'k'}(\lambda)\delta n^m_{l'k'} = 0 , \tag{4.11}$$

where

$$A^m_{lkl'k'}(\lambda) = \delta_{lk}\delta_{l'k'} - 2\lambda V^m_{lkl'k'}(\lambda) ,$$

$$V^m_{lkl'k'}(\lambda) = (C_l^m C_{l'}^m)^{1/2} \int_0^1 du \int_0^{\zeta_{\max}} d\zeta\, n_e^0(\zeta,u;\lambda) P_l^{|m|}(u) \times P_{l'}^{|m|}(u)\Psi_k(\zeta,u) \times \Psi_{k'}(\zeta,u) ,$$

and $|m| \le l,l' \le l_{\max}$, $0 \le k,k' \le k_{\max}$. Matrices (A^m) are symmetric and can be diagonalized. The mth bifurcation point is defined as the solution of equation $d^m_{\min}(\lambda)=0$, where $d^m_{\min}(\lambda)$ denotes the minimal eigenvalue of (A^m). We expect that λ_c^s corresponds to $m=2$. In Fig. 6 we plot $d^{m=2}_{\min}(\lambda)$ for the following three sizes of matrix $(A^{m=2})$: (1) $l_{\max}=4$, $k_{\max}=3$, (2) $l_{\max}=10$, $k_{\max}=5$, and (3) $l_{\max}=10$, $k_{\max}=15$. As expected, the increase in the matrix size shifts λ_c^s to the left. We find, however, that further enlargement of the matrix does not change λ_c^s significantly and it can be estimated at $\lambda_c^s \approx 3.55$. This value is well below $\lambda_I = 4.19$ at which the bulk transition to the nematic phase occurs. We also note that our previous rough estimate of λ_c^s is quite close to the value obtained from the rigorous bifurcation analysis. The above results show that the surface phase transition in which the uniaxial symmetry of the system is broken does occur. However, we have not attempted to extend the bifurcation analysis to the next order to determine the order of the surface transition.

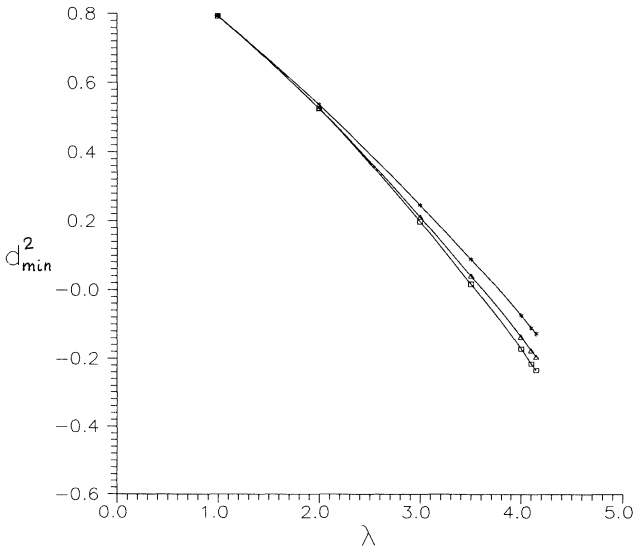

FIG. 6. Minimal eigenvalue of the matrix $(A^{m=2})$ vs the bulk density λ for (1) $l_{\max}=4$, $k_{\max}=3$ (asterisks), (2) $l_{\max}=10$, $k_{\max}=5$ (triangles), and (3) $l_{\max}=10$, $k_{\max}=15$ (squares). The bifurcation point corresponds to $d^2_{\min}(\lambda)=0$.

V. DISCUSSION

We have studied ordering of hard needles close to a hard and structureless wall. The density of the system is measured in units of L^2D which means that the packing fraction tends to zero when $L/D \to \infty$. Despite a vanishingly small packing fraction, the system exhibits the nematic-isotropic transition. Therefore it is a convenient model system to study ordering of anisotropic particles at interfaces, such as the nematic-isotropic or the nematogen-wall interface. In the latter case, we can further distinguish two situations: (1) the bulk phase is isotropic and (2) the bulk phase is nematic. The first situation is simpler as then the one-particle distribution function has uniaxial symmetry with respect to the normal to the wall. However, as we have seen it is true only if the parameter λ is sufficiently below its value at the nematic-isotropic transition.

It is interesting to compare the density profiles $\rho(z)$ for hard needles, obtained in the uniaxial case (see Fig. 1), with a typical $\rho(z)$ for hard spheres at a hard wall. The former are structureless apart from a maximum in a form of cusp at $z=L/2$. The cusp results from the restricted rotational freedom of the particle close to the wall. Also for systems of finite packing fraction the same effect may cause a discontinuity in the first derivative of the density profile. Then, however, the discontinuity may not coincide with the maximum. Apart from the vanishing packing fraction, the lack of oscillations in $\rho(z)$ may be caused by averaging over the orientational degrees of freedom. We observe that the contact density, $\rho(0^+)$, is equal to zero for hard needles while for hard spheres it is finite and related to the pressure by the sum rule. A closer analogy with hard spheres can be obtained if one considers the density of the ends, $\rho_e(\zeta)$. Then the pressure sum rule can be expressed as $\rho_e(0^+)=\beta p$. Because we use an approximate Ω, it is not obvious that the above condition is satisfied by solutions of integral equation (2.3). To prove that it is true, we can use similar argumentation of that of van Swol and Henderson [18]. They showed that for a hard-sphere fluid near a wall, the pressure sum rule is obeyed by any weighted density approximation (WDA) with a spatially varying weighted density. The Onsager approximation in the hard-sphere limit belongs formally to the same class of approximation as WDA. The extension of the proof to a system of hard anisotropic particles is straightforward. Therefore, any solution of Eq. (2.3) should satisfy the pressure sum rule.

We verify our numerical results calculating the deviation from this rule, i.e., $\Delta = \rho_e(0^+) - \beta p$. For $\lambda < 3$, Δ is small which means that the numerical solution is consistent with the pressure sum rule. However, for $\lambda > 3$ a more significant discrepancy occurs. This results from a limited accuracy of the numerical procedure. We solve a nonlinear integral equation for a function of two variables and, in addition, the solution is expected to have rather unusual features. Note that $\rho_e(\zeta,\omega)$ is very steep in the neighborhood of the maximum [see Eqs. (2.15)]. At the maximum the slope becomes infinite and the divergence is logarithmic. These features of the distribution function result from the limiting procedure of mak-

ing the particles infinitely thin.

The final remark concerns the validity of the Onsager approximation in the limit $L/D \to \infty$. For a spatially uniform system, one can examine the reduced virial coefficients defined as $B_n(\text{reduced}) = B_n / B_2^{n-1}$ to verify the condition $B_n(\text{reduced}) << 1$ for $L/D \to \infty$. Only if this condition is satisfied is the Onsager theory of the nematic-isotropic transition self-consistent. Frenkel's [19] direct numerical calculation of the third through fifth virial coefficients of hard spherocylinders with L/D between 1 and 10^6 shows that $B_n(\text{reduced})$, $n = 3,4,5$, are very small when L/D is very large. This result applies to the isotropic phase, however. Certainly, the Onsager approximation breaks down when all spherocylinders are almost parallel, i.e., close to the nematic–smectic-A transition. Then the contribution of the third-order term of the virial expansion to the free energy is important and significantly changes the density at which the nematic–smectic-A transition occurs [20]. There is, however, an important difference between both transitions. The nematic-isotropic transition occurs at a finite value of $\lambda \sim B_2\rho$, which means zero packing fraction in the limit $L/D \to \infty$. On the contrary, the nematic–smectic-A transition occurs at a finite packing fraction, which corresponds to $\lambda \to \infty$ when $L/D \to \infty$.

The wall–hard-needle system, studied in this paper, has zero packing fraction and λ is below its value at the nematic-isotropic transition. For this reason we would expect the Onsager approximation to work well also in this case. On the other hand, the reduced dimensionality near the hard wall may make the approximation less reliable. At present we have no definite answer to the question about importance of higher-order terms in the virial expansion and further investigations are necessary.

ACKNOWLEDGMENTS

The author would like to thank T. J. Sluckin for a helpful discussion. A part of this work was supported by the SERC (U.K.).

[1] B. Jérôme, Rep. Prog. Phys. **54**, 391 (1991).
[2] T. J. Sluckin and A. Poniewierski, in *Fluid Interfacial Phenomena*, edited by C. A. Croxton (Wiley, New York, 1986), Chap. 5.
[3] P. G. de Gennes, Mol. Cryst. Liq. Cryst. **12**, 193 (1971).
[4] P. Sheng, Phys. Rev. A **26**, 1610 (1982).
[5] T. J. Sluckin and A. Poniewierski, Phys. Rev. Lett. **55**, 2907 (1985).
[6] A. K. Sen and D. E. Sullivan, Phys. Rev. A **35**, 1391 (1987).
[7] S. Faetti and V. Palleschi, Phys. Rev. A **30**, 3241 (1984).
[8] B. M. Ocko, A. Braslau, P. S. Pershan, J. Als-Nielsen, and M. Deutsch, Phys. Rev. Lett. **57**, 94 (1986).
[9] R. Holyst and A. Poniewierski, Phys. Rev. A **38**, 1527 (1988).
[10] B. G. Moore and W. E. McMullen, Phys. Rev. A **42**, 6042 (1990); W. E. McMullen, *ibid.* **38**, 6384 (1988); Z. Y. Chen and J. Noolandi, *ibid.* **45**, 2389 (1992).
[11] J. V. Selinger and D. R. Nelson, Phys. Rev. A **37**, 1736 (1988).
[12] Z. Pawlowska, G. F. Kventsel, and T. J. Sluckin, Phys. Rev. A **36**, 992 (1987).
[13] L. Onsager, Ann. N.Y. Acad. Sci. **51**, 627 (1949).
[14] A. Poniewierski and R. Holyst, Phys. Rev. A **38**, 3721 (1988).
[15] G. Stell, *The Equilibrium Theory of Classical Fluids* (Benjamin, New York, 1964).
[16] R. Holyst, Mol. Phys. **68**, 391 (1989).
[17] C. P. Fan and M. J. Stephen, Phys. Rev. Lett. **25**, 500 (1970).
[18] F. van Swol and J. Henderson, Phys. Rev. A **40**, 2567 (1989).
[19] D. Frenkel, J. Phys. Chem. **91**, 4912 (1987); **92**, 5314(E) (1988).
[20] A. Poniewierski, Phys. Rev. A **45**, 5605 (1992).